

CAROTID WALL SEGMENTATION AND *IMT* MEASUREMENT IN LONGITUDINAL ULTRASOUND IMAGES USING MORPHOLOGICAL APPROACH

Filippo Molinari¹, Member IEEE, Guang Zeng², Jasjit S. Suri³, Sr. Member IEEE, Fellow AIMBE

¹Biolab, Department of Electronics, Politecnico di Torino, Torino, Italy

²Mayo Clinic, Rochester, MN, USA

³Aff. Idaho State University, Pocatello, ID and Biomedical Technologies Inc., Denver, CO, USA

ABSTRACT

We developed a completely automated technique for carotid wall segmentation and intima – media thickness (*IMT*) measurement in ultrasound images based on the watershed transform. Morphological operators are used to extract the foreground markers for performing marker-based watershed segmentation. The watershed basin containing the carotid artery is automatically extracted. The far wall of the artery is segmented in order to measure *IMT*.

Results obtained on 200 images were validated against human tracings. Performance was compared to a previously developed automated algorithm. Watershed technique outperformed the previous architecture and resulted in a *IMT* measurement error equal to 2.36 ± 2.76 pixels (0.15 ± 0.17 mm).

Index Terms— watershed transform, carotid segmentation, intima-media thickness (*IMT*), validation, ultrasound

1. INTRODUCTION

According to the World Health Organization studies, atherosclerosis is one of the major life threatening diseases expected to cause one-third of all global deaths by 2040. Early diagnosis is crucial to decrease the associated risk of cardiovascular diseases. The most investigated effect of atherosclerosis is the thickening of the intima-media layers (*IMT*) of the arteries' wall.

Ultrasound imaging is the most used methodology for *IMT* measurement and patient follow-up, due to its low cost, safety, portability, repeatability, and effectiveness. Unfortunately, ultrasound exams are operator-dependent. To overcome the subjectivity of *IMT* measurement made by sonographers, computer methods have been proposed to perform automated measurements. Most of such computer-based approaches require a certain degree of user interaction to locate the artery in the image or to start the segmentation process.

In 2007, we developed a first user-independent algorithm for segmenting the common carotid artery (CCA) wall in longitudinal ultrasound B-Mode images [1]. *IMT*

performance measure was beating the standard (validated against human measurements) and was lower than 40 ± 35 μm against a nominal *IMT* value of about 850 μm . However, our approach suffered from a high sensitivity to noise, which resulted in a failure rate of about 8% of the processed images. Also, the computational cost was high and unsuitable to real-time implementation. A further approach [2] improved speed and robustness to noise, but did not significantly improved measurement performance.

In this paper, we describe a carotid wall segmentation strategy and *IMT* measurement based on the watershed transform of ultrasound images. The rationale was to evaluate the effectiveness of the morphological characteristics of the watershed in carotid ultrasound segmentation. We validated the performance against human tracings and compared with a previously algorithm we proposed in 2009.

2. MATERIALS AND METHODS

2.1 Watershed segmentation strategy

We used marker-based watershed transform to perform image segmentation. The use of markers is essential to avoid over-segmentation caused by the relative high noise of the ultrasound images [3]. Markers are the initial flooding points, so that each marker starts at the watershed basins. We adopted morphological operators (erosion and reconstruction) to individuate the foreground markers. Figure 1 represents the overall watershed segmentation strategy. The original image (fig. 1.A) was first eroded by using a 12 pixel disk-shaped structuring element (fig. 1.B). This step ensured attenuation of noisy and small portions of the image. The image was then reconstructed against the original one (fig. 1.C) and further threshold was applied using Otsu's method (fig. 1.D). The white areas resulting from the thresholding were used to perform the marker-based watershed segmentation. The result for the image in fig. 1.A is reported by fig. 1.E, where each color represents a watershed basin. Fig. 1.F reports the basins overlaid to the original image. It can be noticed that the CCA is recognized in a unique watershed region that comprises the artery lumen and the walls.

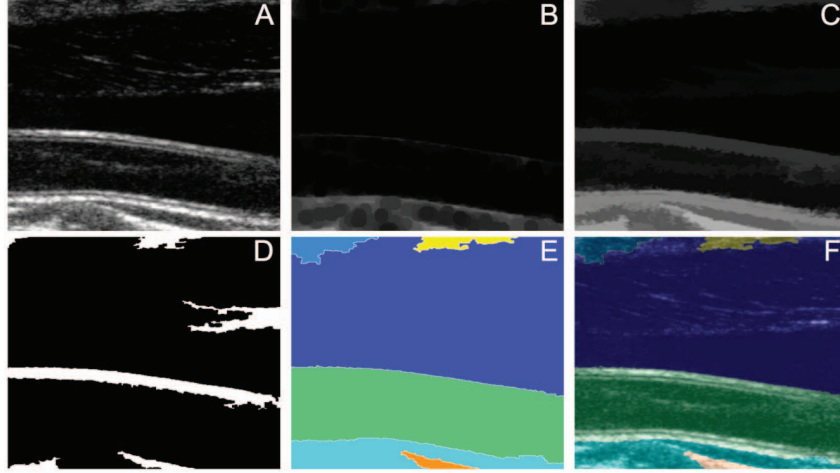


Figure 1. Representation of the watershed-based segmentation for CCA ultrasound images. The original image (A) is first eroded by using a disk-shaped structuring element (B) and then reconstructed against the original image (C). The reconstructed image is thresholded and the above-threshold regions correspond to the markers (D). Fig. E reports the color-coded watershed segmentation. Fig. F reports the watershed basins overlaid to the original image.

2.2 Automatic Common Carotid Artery Recognition

Among the basins obtained by the watershed transform, we had to automatically select the one comprising the CCA. We developed a methodology that specifically searches for the artery lumen, which is a dark and relatively homogeneous zone.

A Canny edge detector was applied to each watershed-segmented region. Grayscale signal envelopes were extracted between the detected edges column-wise in the original image. Along the extracted signal envelope, we determined whether points belonged to lumen region by applying a predefined threshold value T_{lumen} (which was calculated by using Otsu's criterion). For each signal envelope, a column lumen region ratio ε was then calculated as the ratio of the number of classified lumen points to the length of the signal envelope. Only when ε was higher than a predefined threshold value ε_T , we saved the corresponding column for the following lumen region ratio calculation. We used a ε_T value equal to 60%. Finally, the lumen region ratio of each watershed-segmented region was simply calculated as $R_{lumen}^i = S_V / S_T$ where S_V is the number of valid signal envelopes and S_T is the total number of signal envelopes.

Conceptually, if a watershed region contained only the artery lumen, the value of R_{lumen}^i would be equal to 1; if it contained only tissue, its value would be ideally zero. The R_{lumen}^i score alone is insufficient to detect the CCA. In fact, some regions containing the jugular vein lumen (indicated by JV in fig. 1.A) may have a high R_{lumen}^i . To overcome this problem, we inserted a further step. For each watershed-region i , we calculated a geometric and an intensity-based feature: i) H_i : the average region height (defined as the

average distance between the upper and bottom boundaries of that region); ii) I_i : the average region intensity. The three features were then combined to form the score E_i , defined as:

$$E_i = R_{lumen}^i \times \frac{255 - I_i}{255} \times \exp\left(\frac{H_i}{H}\right) \quad (2)$$

where H is the image height. The region containing the CCA was selected as the one with the greater E_i value.

Figure 2 reports the E_i values for the segmented image in fig. 1.A. It can be observed that the region relative to the CCA is characterized by a greater score than the others ($E_5 = 1.908$).

2.3. IMT estimation

We hypothesized that the watershed basin contained the entire CCA, so that the upper boundary of the basin was in correspondence the CCA near wall, and the bottom boundary was in correspondence of the CCA far wall. We traced a ROI starting from the bottom of the basin, which had the same width of the basin and had a height equal to 40 pixels. Since we worked with images having an axial resolution of $62.5\mu\text{m}$, 50 pixels correspond to 3.125mm . This value ensured a ROI comprising the entire far wall and a portion of the artery lumen. The ROI was then considered column-wise. We processed the profile of each column by using a fuzzy *K-means* classifier, which was initialized by the intensity values. The classifier assigned the pixels to three clusters: i) artery lumen (i.e., low intensity pixels); ii) intima and media layers (i.e., average intensity pixels), and iii) adventitia layer (i.e., high intensity pixels). The point at the transition between clusters i) and ii) was considered as

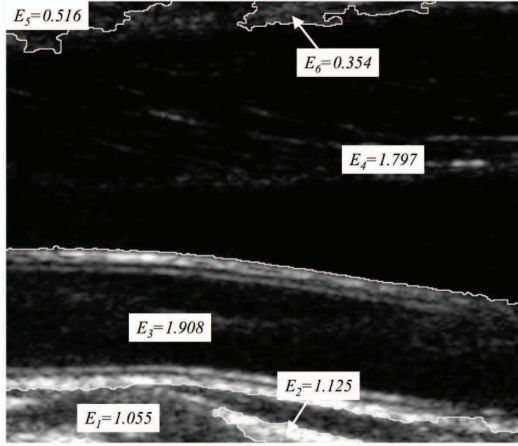


Figure 2. Scoring of the six watershed basins. The CCA is recognized as the basin with the higher score (E_3).

the marker of the *LI* interface; whereas the point at the transition between the clusters ii) and iii) was the marker of the *MA* interface. All the columns in which the classifier could not find the three clusters were discarded. The sequence of the *LI* and *MA* markers constituted the final profiles. Figure 3.A reports a sample of automatically traced *LI* and *MA* boundaries.

The *IMT* was then calculated as the distance between the *LI* and the *MA* profiles. We used the polyline distance method (PDM) to compute the distance between the two boundaries. Details about PDM computation can be found in [4]. By summarizing, given two boundaries B_1 and B_2 , let $d_{1,2}$ be the lower distance between the vertices of B_1 and the segments of B_2 , and let $d_{2,1}$ be the lower distance between the vertices of B_2 and the segments of B_1 . The PDM is defined as the minimum between d_{12} and d_{21} . We used this metrics since it is insensitive to the number of points constituting the boundaries. Hence, *IMT* was calculated as the PDM between *LI* and *MA*.

2.4 Image Database and Performance Metric

We tested our watershed-based technique on a sample database consisting of 200 B-Mode ultrasound images acquired during clinical examinations at the Gradenigo Hospital of Torino, Italy. The images were relative to 150 subjects, aging 69 ± 16 years (range: 50-83). Images were acquired by using an ATLHDI5000 (ATL, Seattle, WA) ultrasound scanner equipped by a 12mm linear probe working at a frequency of 10 MHz. The axial resolution of the images was fixed to $62.5 \mu\text{m}/\text{pixel}$. All the images were transferred to a computer via a DICOM port in lossless format, after logarithmic compression and discretization on 8 bits. Three expert operators (a cardiologist, a neurologist, and a radiology technician) independently segmented the images by using a graphical user interface we previously

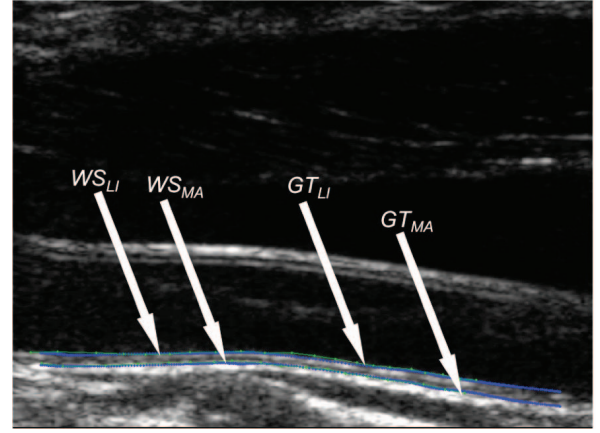


Figure 3. Final segmentation obtained by using the watershed technique. The blue lines depict the watershed (*WS*) *LI* and *MA* profiles; the green lines depict the ground truth (*GT*).

developed. The average segmentation was considered as the Ground Truth (*GT*).

We compared the performance of the watershed technique with those of a methodology we previously developed in 2009 [2]. Briefly, we proposed an integrated approach consisting of feature extraction, fitting and classification, which could automatically detect the CCA. Detection was based on features of the image, by modeling the artery as a continuous dark region (the lumen) surrounded by bright stripes (the walls). We named that technique as *CALEXia* (Completely Automated Layers EXtraction based on integrated approach). After CCA tracing, *CALEXia* performed *IMT* measurement using the same fuzzy *K-means* classifier described in section 2.3. Performance metrics relied on PDM. We calculated the PDM for the *LI* and *MA* boundaries between watershed and *GT* and between *CALEXia* and *GT*.

3. RESULTS AND DISCUSSION

3.1 Segmentation and IMT Performance

Of the 200 images, the watershed transform passed the test on 181 images while failing on 19 cases (9.5%). In these images, due to excessive noise, the CCA was split in two or more basins. This precluded the automated CCA recognition and, therefore, segmentation. These images were discarded. *CALEXia*, on the same database, failed in processing 20 images (10%). Such failure rates are comparable to that of other consolidated automated techniques [1,2] and represent an acceptable performance when working without any user interaction. At the end, we evaluated the performance on the remaining 165 common images.

Table I reports the performance of the watershed (*WatShed*) technique compared to *CALEXia* and *GT*. *WatShed* technique outperforms *CALEXia* both in *LI* and in

MA segmentation. *WatShed* segmentation errors were equal to 0.41 ± 0.56 mm for the *LI* and 0.33 ± 0.49 mm for the *MA* boundary. The *IMT* measurement error was equal to 2.36 ± 2.76 pixels (0.15 ± 0.17 mm) for *WatShed* and 5.1 ± 3.6 pixels (0.32 ± 0.23 mm) for *CALEXia*. The relatively large standard deviation of the system errors is justified by the fact that our database incorporated healthy as well as pathologic images, acquired by different operators using different scanner settings. The images in the dataset are therefore characterized by different noise levels; thus, a significant performance variability was expected.

A direct comparison of such performance with respect to previously developed techniques is not straightforward. Most of the best performing techniques for *IMT* measurement can be considered as computer aids and usually require user interaction. User-dependent algorithms can offer *IMT* measurement errors lower than $10 \mu\text{m}$ [5], whereas user-independent approaches offer performances three or four time worse (*IMT* measurement error can be as high as $50 \mu\text{m}$) [1]. When tested on the same image dataset, the algorithm by Faita et al. [5] showed a *IMT* bias equal to 1.88 ± 1.01 pixels, thus neatly lower than our automated techniques. We anticipate the development of a high-performance *IMT* measurement technique by Greedy fusion of our automated methods, in order to reach same performance of user-dependent methods.

Previously published results were validated using the mean absolute distance as performance metric. Such metric lead to biased results when the boundaries are not parallel. In this case, the validation in terms of *IMT* measurement error could be erratic. PDM is also insensible to the number of points of the boundaries, thus constituting a more robust metric. We will validate PDM against human measurements by comparing to repeated manual estimations made by different expert sonographers.

WatShed technique outperformed *CALEXia* both in *LI* and *MA* segmentation and *IMT* measurement. It must be noted, however, that the segmentation errors on the *LI* and *MA* boundaries are still too high and not suitable to clinical use. The *LI* interface is the most critical one.

Table I – Performance of the *WatShed* and *CALEXia* techniques compared to *GT*. Errors are expressed as PDM between boundaries. Unit is pixels.

	<i>WatShed</i> vs <i>GT</i>	<i>CALEXia</i> vs <i>GT</i>
<i>LI</i> segm error	6.6 ± 8.9	13.2 ± 6.6
<i>MA</i> segm error	5.2 ± 7.8	7.9 ± 7.8
<i>IMT</i> error	2.36 ± 2.76	5.1 ± 3.6

3.2 *WatShed* Advantages and Limitations

The herein proposed strategy watershed-based offers some advantages over previously developed techniques. First, the CCA localization is effective and fully automated. In no images, the CCA was confounded with the JV. Second, the overall computational cost is relatively low. The average

segmentation time was equal to 18 ± 3 s on a dual 2.5 GHz PowerPc with 8 GB of RAM in a Matlab framework.

However, images with low signal-to-noise ratio still represent a limit to this approach. In presence of high noise, the watershed tends to over-segment the image, resulting in the impossibility of locating the CCA. The average numbers of basins in correctly processed images is 6, whereas in incorrectly processed images it is 9. Ad-hoc strategies should be implemented to effectively reduce noise and strengthen the watershed performance.

We tested several approaches and found that the erosion and reconstruction with a 12 pixels disk element is the optimal choice. Smaller elements would cause over-segmentation; bigger would cause under-segmentation (*i.e.*, all the image is assigned to a single basin). Currently, we are working in the field of improving the *IMT* measurement procedure.

5. CONCLUSIONS

We have developed a watershed-based technique for the common carotid artery segmentation and *IMT* measurement in longitudinal ultrasound images. This technique represents a novel architecture in automated carotid artery location and segmentation, based on morphological operators and fuzzy logic classification. Results showed that tracings may have scope of improvement, especially in the segmentation of the lumen-intima interface.

Nevertheless, this new technique outperformed a previously developed methodology and can therefore constitute a further step in high-performance automated carotid images processing.

5. REFERENCES

- [1] S. Delsanto, F. Molinari, P. Giustetto, et al. "Characterization of a completely user-independent algorithm for carotid artery segmentation in 2-D ultrasound images", *IEEE Trans Instrum Meas*, vol. 4, pp. 1265-1274, 2007.
- [2] F. Molinari, G. Zeng, J.S. Suri, "An Integrated approach to computer-based automated tracing and its validation for 200 common carotid arterial wall ultrasound images: a new technique", *J Ultras Med*, (in press).
- [3] A. Krivanek, M. Sonka, "Ovarian ultrasound image analysis: follicle segmentation", *IEEE Trans Med Imaging*, vol. 17(6), pp. 934-944, 1998.
- [4] J.S. Suri, R.M. Haralick, F.H. Sheehan, "Greedy algorithm for error correction in automatically produced boundaries from low contrast ventriculograms", *Pattern Analysis & Applications*, vol. 3, pp. 39-60, 2000.
- [5] F. Faita, V. Gemignani, E. Bianchini, et al. "Real-time measurement system for evaluation of the carotid intima-media thickness with a robust edge operator", *J Ultras Med*, vol. 27, pp. 1353-1361, 2008.